ISBN: 978-3-95450-247-9 ISSN: 2673-5490 doi: 10.18429/JACoW-IPAC2024-THPC67

UPDATED ANALYSIS OF BEAM HALO MEASUREMENTS IN LHC RUN 2 AND RUN 3*

M. Rakic[1,2,†] , M. Giovannozzi [2], P. Hermes[2], D. Mirarchi[2], C. E. Montanari[2,3], K. Paraschou[2], S. Redaelli[2], B. Salvachua[2], S. Morales Vigo[2]
[1]Ecole Polytechnique Fédérale de Lausanne, Lausanne, Switzerland
[2]European Organization for Nuclear Research, Meyrin, Switzerland
[3]University of Manchester, Manchester, UK

Abstract

Measurements of the transverse beam halo in the Large Hadron Collider (LHC) provide crucial input for the performance evaluation of the collimation configuration in the High-Luminosity LHC (HL-LHC) era. Such measurements are carried out in various phases of the LHC operational cycle by scraping the beam with movable collimators. Understanding the halo population and halo formation mechanisms is crucial for optimising accelerator performance. Analysis of collimator scan data allows the evaluation of future needs for active halo depletion mechanisms at the HL-LHC, or other ways of mitigating halo-related risks to machine availability and protection. This contribution analyses the LHC Run 2 (2015-2018) and Run 3 (started in 2022) measurements using measured bunch-by-bunch beam intensity data. Different beam parameters are explored by profiting from upgraded beam parameters in the LHC injector complex.

INTRODUCTION

The CERN Large Hadron Collider (LHC) is a circular accelerator, approximately 27 km in circumference, accelerating and colliding two proton or heavy-ion beams at energies of up to 7.0 TeV per beam particle. The LHC was designed to store a total beam energy of 362 MJ, which has already been surpassed in Run 3, reaching energies of 435 MJ. Such high beam intensities can potentially damage the machine if lost in an uncontrolled manner. Even small losses can lead to quenching of its superconducting magnets, leading to interruption of machine operation and loss of operational efficiency. Therefore, the LHC is protected by a multistage collimation system [1–3]. Primary (TCP) collimators are directly exposed to the circulating main beam and are located in the betatron collimation insertion region IR7 and momentum collimation region in IR3. All other collimators are retracted from the TCPs. Details on all types of collimators in the LHC are given in [4, 5].

In the following, we define the ensemble of beam particles above a transverse amplitude of 3 σ_N as the transverse beam halo, where σ_N is the beam size calculated for the nominal normalised LHC beam emittance of 3.5 µm rad. The beam halo population in the LHC is usually measured using collimator scans, where the jaws of a TCP are moved inward in steps. This procedure is a destructive method to the beam and requires dedicated beam time and elaborate post-processing. In the analysis of the scraping data, the fraction of particles removed as a function of the position of the collimator jaw can be extracted using measurements from beam current transformers (BCT). Two types of BCT are available in the LHC: a direct-current transformer (BCT-DC) that measures the intensity of the entire beam; a fast-response transformer (BCT-FR) that measures the intensity of each bunch in the beam. Alternatively, a set of beam loss monitor (BLM) signals can be used to estimate the amount of protons lost at each collimator step. The BLMs are ionisation chambers that measure the flux of secondary particles generated by protons interacting with matter, for example, when particles are lost in collimators or other accelerator equipment. The BLM signals close to the collimators, measured in Gy/s, can be calibrated to obtain absolute proton loss rates in protons/s [6–9].

Beam measurements in LHC Run 2 (2015–2018) and Run 3 (started in 2022) have shown that the beam halo population can considerably exceed that of a Gaussian distribution [7, 10], with up to 5 % of the total beam intensity in the beam halo. With the HL-LHC upgrade, the stored beam energy will be increased to 680 MJ [5]. When scaling the LHC observations to the HL-LHC, the beam halo could store up to 35 MJ, with the potential to damage the collimation system during fast failures, such as sudden orbit jitters. Understanding the population and evolution of the transverse beam halo in the different phases of the LHC operational cycle is therefore crucial to evaluate the associated risk. In this article, we compare the LHC halo population measurements from Run 2 with the Run 3 measurements, the latter carried out after the LHC Injector Upgrade (LIU) [11] which are expected to be more indicative of the conditions in HL-LHC.

COLLIMATOR SCRAPING ANALYSIS

For beam-halo measurements with collimator scraping, horizontal (H) and vertical (V) TCPs in IR7 are used, starting at their nominal position of 5 σ_N at the top energy of 6.8 TeV in LHC Run 2 and 3 [12]. Measurements were performed with operational physics beams. Before scraping, the collimator jaws are centred around the beam [13], and then the TCP jaws are moved closer to the beam centre in steps of roughly 10 µm (~ 0.05 σ_N) every few seconds. Measurement opportunities are limited because scraping is destructive to the beam. Intensity changes derived from the BCT intensity signal before and after each collimator step

* Work supported by the HL-LHC project.
† milica.rakic@cern.ch

ISBN: 978-3-95450-247-9 ISSN: 2673-5490 doi: 10.18429/JACoW-IPAC2024-THPC67

allow for the calculation of the amount of particles removed at each position. The cumulative stored halo content is calculated from these signals as a function of the transverse beam amplitude.

Each collimator is equipped with a BLM. To determine the number of lost charges, a calibration is applied to the measured signals of a set of BLMs [6, 14]. Two types of BLM calibrations, proposed in [9], were studied. One provides the total lost intensity per second (global calibration) and the other provides the loss decomposition per plane. The analysis with both approaches has produced results that are in very good agreement. The analysis and calibration process is described in [10, 14].

Comparison of Halo Content in Run 2 and Run 3

The summary of the halo population derived from the BCT-DC and BLM data, during the halo measurements in Run 2 and Run 3, is presented in Table 1. The measured halo is reported at the transverse positions of 3.0 σ_N and 3.5 σ_N together with what is expected for a Gaussian distribution. The halo content exceeds that of a Gaussian in both runs, although to a lesser extent in Run 3. The data also show a significant variation in the halo content from fill to fill.

We conclude that a single-halo model cannot comprehensively describe the observed halo. Instead, a method based on multiple models would be better suited. We consider the possibilities of constructing the halo based on a model of the entire beam (sum of all bunches), employing different probability distributions, or as a bunch-resolved estimation. The bunch-by-bunch halo measurement results are discussed in further detail in later sections of this paper.

Table 1: Halo population across Run 2 and Run 3 scraping tests. The halo, given in percent of the total beam intensity, is shown at different betatron amplitudes and compared to a Gaussian distribution (Gauss [%]).

TCP [σ_N]	Gauss [%]	Run 2 [%]	Run 3 [%]
3.0	0.3	0.2 - 4.0	0.2 - 1.2
3.5	0.05	0.2 - 2.0	0.05 - 1.5

Comparison of BLM and BCT Halo Measurements

The halo population obtained from the analysis of the data collected in a single scraping measurement carried out during LHC Run 3 is shown in Figure 1. It corresponds to a horizontal scraping of LHC Beam 1 (B1). The halo population calculated from the BCT signal is coloured purple, and from the BLM global calibration is coloured blue. The Gaussian distribution corresponding to the nominal emittance ϵ_N is drawn as a solid red line, while the Gaussian corresponding to the emittance value measured during this measurement (1.5 µm rad) is drawn as a dashed red line. The uncertainty of the BCT signal is evaluated from the minimal and maximal signals observed at every collimator position. The uncertainty of the BLM signal is propagated from the calibration error and the noise of the BLM signal without beams.

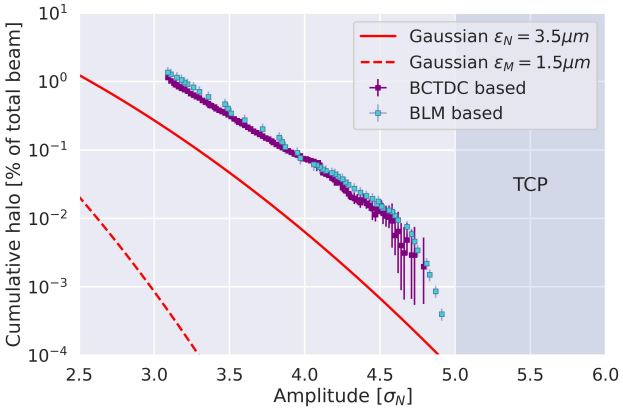

Figure 1: Halo population as a function of the amplitude from the bunch centre in B1H, during a scraping measurement of Run 3 fill 8387.

Comparing the BCT and BLM based halo estimates, we can see that at high transverse amplitudes and low beam intensities, the BCT-based estimate is noisier than that based on the BLM signal. This can be explained by the sensitivity of the BLMs being 4 orders higher than that of the BCT [10]. This observation is important for HL-LHC related measurements. In the HL-LHC configuration, the TCP half-gap will potentially be set at 8.5 σ_{HL} [15] (with the HL-LHC normalized emittance of ϵ_{HL} = 2.5 µm), which is beyond the amplitudes probed in the measurements performed so far. In these transverse regions, we expect smaller halo populations, such that only BLM-based measurements could be used.

In conclusion, the estimate of the halo content is consistent between the two methods employed when applied in regions with sufficient beam intensity. The same conclusion was drawn from the remaining measurements throughout Run 2 and Run 3, which are not presented in detail here.

Bunch-by-bunch Halo Reconstruction

The halo population can be reconstructed for each bunch in a similar manner by using the bunch-sensitive BCT-FR signal. In Fig. 2, the halo content above 3.5 σ_N of each bunch is shown as a function of the bucket slot for a high-intensity fill in Run 3. The depicted halo population varies across the bunch trains, showing a consistent pattern with lower halo content at the head of each train and an increase toward the tail of the train.

Following these findings, it was hypothesised that bunches with a larger halo population could have larger initial emittances. To study a potential correlation, the bunch-by-bunch emittance before collimator scraping, measured with the beam synchrotron radiation telescope (BSRT) [16], was compared with the bunch-halo population for all available Run 3 measurements (Run 2 BSRT emittance data are not available). A weighted linear regression analysis was performed and the Pearson correlation coefficient was calculated, using the *Python Statsmodels* package [17]. The weight of the

ISBN: 978-3-95450-247-9 ISSN: 2673-5490 doi: 10.18429/JACoW-IPAC2024-THPC67

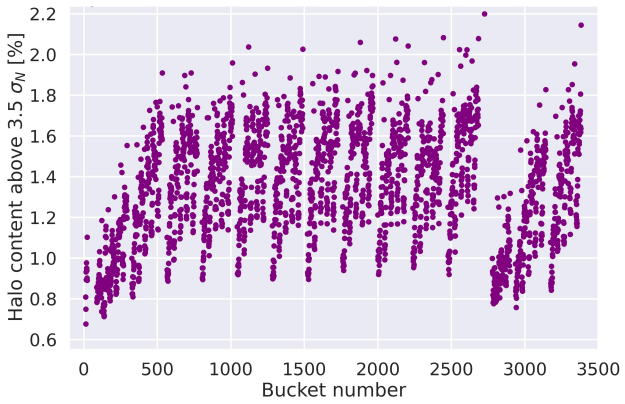

Figure 2: Measured B1H halo content for individual bunches during the Run 3 high-intensity fill 8387 at the final position of the TCP of $3.5\sigma_N$ as a function of the bucket number.

fit was given as the intensity of the bunch before scraping, normalised to the highest intensity of the bunch across the bunches $I_{bunch}/\max(I_{bunch})$.

Figure 3 shows the results of this analysis for selected halo measurements in LHC Run 3, performed after several hours of stable (colliding) beams. One measurement with 1200 bunches (Fill 8313, non-colliding) and 2462 bunches (Fill 8387, colliding), both with 25 ns bunch spacing and at $\beta^* = 30$ cm [18]. The colour reflects the intensity of the bunch. The results of the analysis are summarised in Table 2 for the four cases with the strongest and weakest correlation identified. The table shows the intercept value α, slope β, p value and R^2 of the linear regression, and the Pearson correlation coefficient ρ (unweighted, thus different from $\sqrt{R^2}$ presented here).

Table 2: Results of regression analysis: intercept α, slope β, p-value, and R^2 value of the regression fit, and the Pearson correlation coefficient ρ.

Fill	Plane	α [%]	β [% µm^{-1}]	p	R^2	ρ
8313	B1H	-2.94	2.66	$\leq 10^{-3}$	0.72	0.87
	B2H	-0.53	0.35	$\leq 10^{-3}$	0.39	0.62
8387	B1H	0.64	0.27	$\leq 10^{-3}$	0.04	0.22
	B1V	0.29	0.18	$\leq 10^{-3}$	0.04	0.19

For the measurement in Fill 8313 (see Fig. 3, top) a strong correlation of $\rho = 0.87$ was found between the measured halo content and the transverse emittance in B1H. For B2H, a moderate correlation of $\rho = 0.62$ was found. For these examples, linear regression seems to describe the relationship very well. It should be noted that the slope of the regression lines for B1H and B2H is different by almost one order of magnitude, indicating that the degree to which the halo content varies with the emittance can be very different, even if a strong correlation is observed. As another example, for Fill 8387 (see Fig. 3, bottom), a weak correlation was found between the initial emittance and the halo content, both for

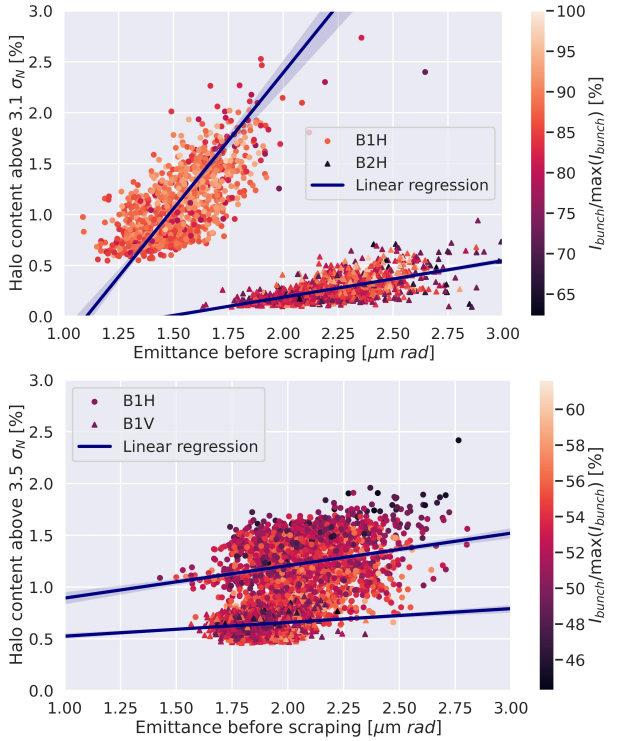

Figure 3: Measured halo content vs. bunch emittance before scraping measured for different planes and beams in Run 3 (Fill 8313 (top) and Fill 8387 (bottom)).

B1H ($\rho = 0.22$) and B1V ($\rho = 0.19$). Although a similar β was found as in B2H for Fill 8313, the linear model has much less explanatory power. Clear conclusions cannot be drawn, as while in some cases the bunch emittance and the halo seem to be correlated, in other cases the correlation is weak. We plan to perform a deeper analysis and expect further insights from future measurements.

CONCLUSIONS

The presented results of Run 3 halo measurements align with previous reports of halo overpopulation. Based on the strong variation of the measured beam halo from fill to fill, more complex halo models than the previously employed double Gaussian model will be explored [19].

The bunch-resolved halo analysis revealed new findings. The halo population was shown to vary from one bunch to another and exhibits a pattern along the bunch trains. Our attempts to explain the pattern by differences in bunch emittance have not resulted in a clear conclusion. In some cases, the halo is indeed correlated with the initial bunch emittance, while for other cases the correlation was weak. More measurements and analyses are needed before a definitive conclusion can be drawn on this matter.

ACKNOWLEDGMENTS

We would like to thank the LHC shift crews for their constant support in these measurements. Furthermore, we express our gratitude to A. Gorzawski for useful discussions.

ISBN: 978-3-95450-247-9 ISSN: 2673-5490 doi: 10.18429/JACoW-IPAC2024-THPC67

REFERENCES

[1] R. W. Assmann *et al.*, "The Final Collimation System for the LHC," in *Proc. EPAC'06*, Edinburgh, UK, 2006, pp. 986–988.

[2] R.W. Assmann, "Collimators and Beam Absorbers for Cleaning and Machine Protection," in *Proc. LHC Project Workshop - Chamonix XIV*, Chamonix, France, 2005, p. 261.

[3] R. Bruce *et al.*, "Simulations and measurements of beam loss patterns at the CERN Large Hadron Collider," *Phys. Rev. Spec. Top. Accel. Beams*, vol. 17, p. 081 004, 2014. doi:10.1103/PhysRevSTAB.17.081004

[4] O. S. Brüning *et al.*, "LHC Design Report," CERN, Tech. Rep., 2004. doi:10.5170/CERN-2004-003-V-1

[5] O. Aberle *et al.*, "High-Luminosity Large Hadron Collider (HL-LHC): Technical Design Report," CERN, Tech. Rep., 2020. doi:10.23731/CYRM-2020-0010

[6] S. M. Vigo *et al.*, "Beam Loss Signal Calibration for the LHC Diamond Detectors During Run 2," in *Proc. IBIC'21*, Pohang, Korea, 2021, pp. 290–293. doi:10.18429/JACoW-IBIC2021-TUPP33

[7] A. Gorzawski *et al.*, "Probing LHC halo dynamics using collimator loss rates at 6.5 TeV," *Phys. Rev. Spec. Top. Accel. Beams*, vol. 23, p. 044 802, 2020.

[8] G. Valentino *et al.*, "Beam diffusion measurements using collimator scans in the LHC," *Phys. Rev. Spec. Top. Accel. Beams*, vol. 16, p. 021 003, 2 2013. doi:10.1103/PhysRevSTAB.16.021003

[9] S. M. Vigo *et al.*, "Beam lifetime monitoring using beam loss monitors during LHC Run 3," presented at IPAC'23, Venice, Italy, May 2023, paper THPL086.

[10] P. Hermes *et al.*, "Collimator Scan Based Beam Halo Measurements in LHC and HL-LHC," in *Proc. IBIC'23*, Saskatoon, Canada, Sep. 2023, paper TU3C03, 2023. doi:10.18429/JACoW-IBIC2023-TU3C03

[11] H. Damerau *et al.*, "LHC Injectors Upgrade, Technical Design Report," CERN, Tech. Rep., 2014, CERN-ACC-2014-0337. doi:10.17181/CERN.7NHR.6HGC

[12] N. Fuster Martinez *et al.*, "Run 2 Collimation Overview," pp. 149–164, 2019. https://cds.cern.ch/record/2750291

[13] G. Valentino *et al.*, "Comparison of LHC Collimator Beam-Based Alignment Centers to BPM-Interpolated Centers," in *Proc. IPAC'12*, New Orleans, LA, USA, May 2012, pp. 2062–2064.

[14] B. Salvachua, "Beam Diagnostics for Studying Beam Losses in the LHC," in *Proc. IBIC'19*, Malmö, Sweden, 2019, pp. 222–228. doi:10.18429/JACoW-IBIC2019-TUA001

[15] R. Tomas Garcia *et al.*, "HL-LHC Run 4 proton operational scenario," CERN, Tech. Rep., 2022. https://cds.cern.ch/record/2803611

[16] R. Jung, F. Méot, and L. Ponce, "LHC proton beam diagnostics using synchrotron radiation," CERN, Tech. Rep., 2004. doi:10.5170/CERN-2004-007

[17] S. Seabold and J. Perktold, "Statsmodels: Econometric and statistical modeling with python," in *9th Python in Science Conference*, 2010.

[18] M. Hostettler, A. Calia, S. Fartoukh, D. Jacquet, and J. Wenninger, "Operational beta* levelling at the LHC in 2022 and beyond," in *Proc. IPAC'23*, Venice, Italy, 2023, pp. 642–645. doi:10.18429/JACoW-IPAC2023-MOPL045

[19] P. Hermes *et al.*, "HL-LHC Beam Dynamics with Hollow Electron Lenses," in *Proc. HB'21*, Batavia, IL, USA, Oct. 2021, paper MOP09, vol. 2021. doi:10.18429/JACoW-HB2021-MOP09